1-1-2005

YBa2Cu3O7 electro-magneto-optic effects in Ba L2,3 X-ray absorption near Tc

Juana Vivó Acrivos
San Jose State University, juana.acrivos@sjsu.edu

$YBa_2Cu_3O_7$ electro magneto-optic effects in Ba $L_{2,3}$ X-ray absorption near T_c

J.V. Acrivos,

San Jose' State University, One Washington Square, San José CA95192-0101

jacrivos@athens.sjsu.edu, Tel: 408 924 4972; Fax 408 924 4945

running title: **$YBa_2Cu_3O_7$ magneto-optic effects near T_c**

Keywords:

cuprate superconductors, X-ray absorption, Alternant Conjugate LCAO-MO

Abstract

The onset of electro magneto-optic effects, observed at the Ba $L_{2,3}$ edges synchrotron X-ray absorption by a $YBa_2Cu_3O_7$ single crystal, 10 K above the transition temperature to superconductivity, $T_c \sim 92$ K is used to identify the role played by the Ba donor layer in the transition to superconductivity in the CuO_2 layers. Negative permeability leads to Faraday rotation of the transmitted beam below T = 112 to 56 K for the 22 μm thick single crystal (**c**-axis orientation of $8\pi/18$ relative to $\boldsymbol{\varepsilon}_{X\text{-rays}}$) and sharp changes in the density of empty final states lead to zero transmitted radiation in an interval ΔE at the given orientation. The temperature dependence: $\Delta E(L_2)$ = 1.4, 3.5 and 3.9 eV while $\Delta E(L_3)$ = 5.3, 6 and 7 eV at T = 92, 74, 63 K respectively, indicates that the width of the empty final states bands increases as T decreases. $\Delta E(L_3)/\Delta E(L_2)$ = 3.8 at 92 K to 1.8 at 63 K, also indicates that the $d_{5/2}$ symmetry bands fill faster than those of $d_{3/2}$ symmetry below T_c, providing the first experimental evidence of unpaired spin-orbit states in the Ba donor layer of a superconductor. These effects, characteristic of ferromagnetic and anti-ferromagnetic materials near a resonance absorption, signal the onset of a Mott transition. The interaction between the layer states is described using 1D conjugate molecular orbitals.

1. Introduction

The purpose of this work is to determine how electro magneto-optic effects [1-5] if present in the layer superconductor $YBa_2Cu_3O_7$ ($YBCO_7$) (Fig. 1a,b) affect the onset of the transition to superconductivity, at temperature T_c [6-11]. The electro magnetic properties of a metal are determined by an unbalance in the population of its spin-orbit split conduction band states. The X-ray absorption spectra, XAS at an element $L_{2,3}$ edges measure the transition probabilities for the excitations:

$(1s)^2(2s)^2(2p_{1/2})^2(2p_{3/2})^4.. \Leftrightarrow (1s)^2(2s)^2(2p_{1/2})(2p_{3/2})^4\ldots (nd_{3/2})$, at the element L_2 edge

$(1s)^2(2s)^2(2p_{1/2})^2(2p_{3/2})^4.. \Leftrightarrow (1s)^2(2s)^2(2p_{1/2})^2(2p_{3/2})^3\ldots (nd_{5/2})$, at the element L_3 edge.

which are split, by spin orbit interactions in the core and in the conduction band state, i.e.,

$$\Delta E_{L2,3} = h\upsilon_{L2} - h\upsilon_{L3} = \Delta E_{\text{final states}} - \Delta E_{\text{core}}. \quad (1)$$

$\Delta E_{L2,3}$ is dominated by the separation of core states, $-\Delta E_{\text{core}} \approx Z^4_{2p,\text{effective}}/32c^2$ Hartree is the relativistic textbook relation for hydrogen like core states [12a]. $Z_{2p,\text{effective}}$ is the 2p electron shielded atomic number (≈ 24 for Cu and ≈ 50 for Ba is estimated from the $L_{2,3}$ edge separation when $\Delta E_{\text{final states}} << 1$) and c is the velocity of light in atomic units. Recent work has shown that the XAS by a $YBCO_7$, 22 μm thick, single crystal at the Ba $L_{2,3}$ edges [6, 7] is enhanced below T = 112 K going from $\mathbf{c}_{\text{axis}} \wedge \boldsymbol{\varepsilon}_{\text{X-ray}} = \pi/2$ to $8\pi/18$ for linearly polarized synchrotron X-rays (Fig. 2). Changes in the components of the index of refraction: $n = 1 - \delta - i\beta$ [text book relation 12b,c] produce a Faraday/Kerr rotation if n_+ and n_- for the right and left the handed components of the incident linearly polarized radiation, are not equal due to electro magnetic interactions in the $L_{2,3}$ edge transitions final states [1, 2]. Since the population of the final states gives rise to the electro magnetic properties, and d-symmetry band states have been associated with superconductivity in $YBCO_7$, the Ba $L_{2,3}$ edge XAS data is used here to ascertain how changes in the $d_{5/2}$, $d_{3/2}$ symmetry empty final states, in the donor layer affect the CuO_2 conduction layer states near T_c.

2. Materials and Methods

The XAS of a 22 μm thick single crystal $YBCO_7$ grown at the IRC for Superconductivity, Cavendish Laboratory [6, 7] were determined in transmission, T geometry (Fig. 1c) near the Ba $L_{2,3}$ edges at the Stanford Radiation Laboratory, SSRL in the earth electro magnetic field. In order to evaluate the components of the complex index of refraction near T_c detailed orientation measurements are required at a synchrotron facility. These experiments report only the variation with temperature of the magneto-optical effects at a single orientation in order to identify how the final states and their occupation vary near T_c. The onset of superconductivity, was determined by the transparency induced by Abrikosov vortices at the Cu K-edge [6, 7, 11]**.**

3. Results

The raw data, corrected only for a linear background subtraction gives the Absorbance for the single crystal at T = 112 K (Fig. 2, insert):

$$A = \mathrm{Ln}\,(I_T/I_0)/\mathrm{Ln}(10)$$

in T geometry (Fig.1c). The ratio A(T)/A(121-112K) for T <112 K indicates up to a threefold enhancement as T decreases below T_c, at the orientation $\mathbf{c}\hat{}\boldsymbol{\varepsilon}_{X\text{-}rays} = 8\pi/18$. The temperature dependence of the interval ΔE where the transmission vanishes, is indicated for the L_2 and L_3 edges respectively (Fig. 2 inserts).

4. Discussion:

The response components of the scattered or transmitted light I_s or I_T respectively from an incident linearly polarized beam, I_0 by atom a in $YBCO_7$ (Fig. 1) are written [12 b,c]:

$$f_a = f_a^{\,0} + f_a' + i\, f_a''. \qquad (2)$$

The matrix elements leading to (2) are the square of the vector potential A^2 acting once on the electron number density $\rho(\mathbf{r})$ to give $f_a^{\,0}$ responsible for Bragg diffraction far from an element

edge, and near an element edge the energy density **j.A** acts twice to give the anomalous Bragg diffraction: f_a' (dispersion) and f_a" (absorption), where **j** is the current density. Electric and magnetic field **E, H** rotations by φ_{Kerr} or $\varphi_{Faraday}$ are observed in I_s or I_T for both ferromagnetic and antiferromagnetic materials[1, 2, 5]:

$$\varphi_{Kerr} = -\Im_m [(n_+ - n_-)/(n_+ n_- - 1)] \text{ with ellipticity } \varepsilon_{Kerr} = -\Re_e[(n_+ - n_-)/(n_+ n_- - 1)]$$

$$\varphi_{Faraday} = [\pi E z/hc \, \Re_e(n_+ - n_-)] \text{ with ellipticity } \varepsilon_{Faraday} = -\tanh[\pi E z/hc \, \Im_m(n_+ - n_-)]. \quad (3)$$

These give rise to an elliptical polarization of the scattered and transmitted beams respectively. A non zero ellipticity, is caused by unequal changes in the complex n_+ and n_- versus photon energy, E, h is Planck constant and z the distance traversed inside the sample. The final density of states at the $L_{2,3}$ edges, respectively is responsible for the changes in δ and the critical angle, $(2\,\delta)^{1/2}$ for external reflection [textbook definition in ref. 12c] leads to sharp decreases/increases in the transmission over an interval ΔE (where the slope of the empty final density of states versus E diverges, i.e., $d\delta/dE \Rightarrow \pm \infty$). The limits determined by ΔE indicate where sharp changes occur in the density of empty final states, related to the L_2 and L_3 band widths. For 20 to 60 nm Fe ferromagnetic films [Fig. 8 ref. 5] $\Delta E(L_3) \sim 2$ eV and $\Delta E(L_2) \sim 0.28$ eV indicate that the empty states band width is 7.2 times greater for $3d_{5/2}$ than for $3d_{3/2}$, suggesting that the latter is the majority occupied band. The experimental results are discussed in three parts:

A. The 22 μm $YBCO_7$ crystal electro magnetic properties determined by Ba $L_{2,3}$ XAS are:

(i) The sharp changes in the index of refraction in the interval ΔE, observed below 112 K, $\Delta E(L_3)/\Delta E(L_2) = 3.8$ at 92 K to 1.7 at 63 K (Fig. 2 Table insert) indicate that the relative widths and/or population of the $d_{5/2}$ and $d_{3/2}$ symmetry final empty states bands have a different temperature dependence which result in different electro magnetic properties versus T.

(ii) The ratio $\Delta E(L_3)/\Delta E(L_2) = 3.8$ near T_c is smaller than that for a ferromagnetic Fe film of 7.2 [8] at room temperature indicating a greater unbalance of spin-orbit states and therefore stronger magnetic properties for the latter. The unequal population of $d_{5/2}$ and $d_{3/2}$ symmetry final states does not distinguish between ferromagnetic and antiferromagnetic properties, but an equal probability for their occupation should obtain $\Delta E(L_3)/\Delta E(L_2) = 1.5$.

(iii) Faraday rotation extends into the extended X-ray absorption, XAFS as indicated by the enhanced absorption over that at 121 K (Fig. 2).

(iv) The unpaired spin states in the donor layer may be the cause and/or consequence of spin defects in the CuO_2 conduction layer states, that can lead to the formation of superconducting pairs at the onset of superconductivity described as follows.

B. The molecular orbital, MO description of the material suggested by the data is:

(i) The wave functions [12a] involved in the transitions are:

Ba initial core states:

$\psi_{Ba,i}$**: 2p$_{3/2}$:** $|3/2,\pm3/2\rangle = Y_{1,\pm1}\uparrow\downarrow R_{2,1}(r_{Ba})$, $|3/2,\pm1/2\rangle = 3^{-1/2}[2^{1/2} Y_{1,0}\uparrow\downarrow + Y_{1,\pm1}\downarrow\uparrow] R_{2,1}(r_{Ba})$

$\psi_{Ba,i}$**: 2p$_{1/2}$:** $|1/2,\pm1/2\rangle = 3^{-1/2}[Y_{1,0}\uparrow\downarrow - 2^{1/2} Y_{1,\pm1}\downarrow\uparrow] R_{2,1}(r_{Ba})$

and empty final band states band containing fractional character of:

$\psi_{Ba,f}$**: 5d$_{5/2}$:** $|5/2,\pm5/2\rangle = Y_{2,\pm2}\uparrow\downarrow R_{5,2}(r_{Ba})$, $|5/2,\pm3/2\rangle = 5^{-1/2}[Y_{2,\pm2}\downarrow\uparrow + 2Y_{2,\pm1}\uparrow\downarrow]R_{5,2}(r_{Ba})$,

$|5/2,\pm1/2\rangle = 15^{-1/2}[3 Y_{2,0}\uparrow\downarrow + 6^{1/2}Y_{2,\pm1}\downarrow\uparrow] R_{5,2}(r_{Ba})$.

$\psi_{Ba.f}$**: 5d$_{3/2}$:** $|3/2,\pm3/2\rangle = 5^{-1/2}[2 Y_{2,\pm2}\downarrow\uparrow - Y_{2,\pm1}\uparrow\downarrow]R_{5,2}(r_{Ba})$,

$|3/2,\pm1/2\rangle = 15^{-1/2}[6^{1/2}Y_{2,0}\uparrow\downarrow - 3Y_{2,\pm1}\downarrow\uparrow] R_{5,2}(r_{Ba})$. (4)

where $Y_{l,m}(r_a,\theta_a,\varphi_a)$ are spherical harmonics, the sub indexes $\uparrow\downarrow$ represent the spin $s_z = \pm1/2$ states and $R_{n,l}(r_a)$ is the radial dependence when (r_a,θ_a,φ_a) are the spherical polar coordinates of the electron relative to atom a. The LCAO-MO extended state wave functions for the $[CuO_2]_n$ conduction layer, obtained by a SCF analysis give the maps of electron density, $\rho_e > (0.1/\text{bohr})^3$

indicating the direction of the extended electron overlap population along O_{3a}:$2p_{ab}$-O_{3b}:$2p_{ab}$ the a,b and a,-b diagonals (Fig. 3 a,b) [13]. These are built with SCF, MO: $\chi_{m,M} = \chi_{m,74}(Cu_4O_4)$ and $\chi_{m',114}(Cu_4O_{12})^{-x}$ (M is the total number of doubly occupied MO and m is the order of increasing energy, $\varepsilon_{m,M}$) where the $\chi_{m,74}$ are doubly degenerate with an overlap population along the ab or a,-b diagonal (Fig. 3a, e.g., m = 53/54, 63,64, etc.). The highest occupied SCF MO, HOMO ρ_e (m =74/75) identifies the direction of electron overlap population at the Fermi level that agrees with the preferred direction of superconductivity along the a,b and a,-b diagonals, determined experimentally by photoemission measurements [14] later. The experimental conduction electron state wave vectors in the first Brillouin Zone, $\mathbf{k}_{\pm} = (k_y,k_x,k_z) = \pm (\pi, \pm\pi, 0)$ are used in a semi empirical tight binding approximation [12 g] of the layers.

(iii) The extended states are usually built with $\mathbf{k}_{\pm}$ and the SCF MO basis [13] (Fig. 3c). Here simple Alternant 1D conjugate orbitals [15] in a lattice with atom coordinates (Fig. 1a,b, 4):

$$\mathbf{R}_{Cu}: (x/a, y/b, z/c) = (n+n_a, n+n_b, 0),$$

$$\mathbf{R}_{O3a}: (n+n_a+½, n+n_b, \delta) \text{ and } \mathbf{R}_{O3b}: (n+n_a , n+n_b- ½, 0.02)$$

$$\text{and donor layers } \mathbf{R}_{Ba/Y}: (n+n_b + ½, n+n_b- ½, 0.16)$$

are used. n_a, n_b = 0, 1, etc. identify the chains, n = 0, 1, .N. $\mathbf{k}_+ = \pm(\pi, \pi, 0)$ obtains the MO:

$$\chi_{O,\, na,nb}\,(\mathbf{r}, \pi, \pi, k_z) = (2N)^{-½}\, i \cos(\pi(n_a + n_b))\, \Sigma_n\, [\psi_O(\mathbf{r}-\mathbf{R}_{O3a}) - \psi_O(\mathbf{r}-\mathbf{R}_{O3b})],$$

$$\chi_{Cu,\, na,nb}\,(\mathbf{r}, \pi, \pi, 0) = N^{½} \cos(\pi(n_a+ n_b))\, \Sigma_n\, \psi_{Cu}(\mathbf{r}-\mathbf{R}_{Cu}),$$

$$\chi_{donor,\, na,nb}\,(\mathbf{r}, \pi, \pi, k_z) = N^{½} \cos(\pi(n_a+n_b))\, \Sigma_n\, \psi_{donor}(\mathbf{r}- \mathbf{R}_{donor}). \qquad (5)$$

N is the total number of Cu sites in a chain and ψ are atomic orbitals. Along the a,-b diagonal, the 1D overlap occurs for $\mathbf{k}_- = \pm (\pi, -\pi, 0)$. However, if $\mathbf{k}_+$ changes to $\mathbf{k}_-$ the O_{3a}:$2p_{ab}$-O3b:$2p_{ab}$ 1D overlap changes direction (Fig. 3c, 4a, b) creating anti-bonding states, which in turn give rise to periodic lattice distortions, PLD.

(iv) A periodic repeat between broken bonds (Fig. 4) creates expansion and compression waves that can be detected by X-ray diffraction, XRD. A 1D PLD with λ_{PLD} = 12 a has been observed in a 50 nm $YBCO_7$ film [a = 4.88 Å in ref. 10] but 4 by 4 PLD can also be explained by the interchange of $\mathbf{k}_+$ changes to $\mathbf{k}_-$ (Fig. 3c). The undistorted 1D chain length determines the conduction electron mean free path in the chain, and the defect unpaired spin states may be the cause and/or the result of the magneto-optic property changes in the Ba donor layer 10 K before the onset to superconductivity. The energy cost for breaking a O_{3a}:$2p_{ab}$-O3b:$2p_{ab}$ bond is estimated from the SCF, LCAO-MO analysis. The difference in ρ_e between $\chi_{54,74}$ and $\chi_{57,74}$ is due to subtle changes in the O_{3a}:$2p_{ab}$-O3b:$2p_{ab}$ overlap population (Fig. 3a). An additional resonance energy, t due to O_{3a}:$2p_{ab}$-O3b:$2p_{ab}$ overlap is possible for $\chi_{54,74}$ but not for $\chi_{57,74}$ and obtains $\varepsilon_{57,74} - \varepsilon_{54,74} = 0.16$ eV ~ 2 t [13]. Also the SCF energy difference $(\varepsilon_{75,74} - \varepsilon_{74,74})/2 = 0.95$ eV between the Cu_4O_4: HOMO and LUMO is due to the difference in ρ_e for $\chi_{74,74}$ and $\chi_{75,74}$: Two Cu:p-like in the HOMO ρ_e symmetry are associated with a d^{10} closed shell, but addition of an electron gives two Cu:d-like in the LUMO ρ_e symmetry, associated with an open d shell. This is in agreement with the higher heat of formation per mole for the $3d^8$ shell oxide, NiO over that for a $3d^{10}$ closed shell oxide, ZnO by 1.2 eV [12f]. The presence of broken O_{3a}:$2p_{ab}$-O3b:$2p_{ab}$ bond defects does not necessarily increase the ground state energy because of the degeneracy introduced by, e.g., $\chi_{54/53,74}$, $\chi_{57/56,74}$,$\chi_{64/63,74}$, $\chi_{66/67,74}$, $\chi_{74/75,74}$ (Fig. 3a) [13, 17]. This suggests that PLD are formed when $\mathbf{k}_-$ and $\mathbf{k}_+$ are interchanged by an excitation of $2t/N \approx 0.16$ eV/N when one O_{3a}:$2p_{ab}$:O_{3b}:$2p_{ab}$ becomes anti-bonding, in a chain of N atoms [15]. These excitations may be introduced at the onset of $YBCO_7$ Ba lattice vibrations at T< 130 K [16], i.e., the $YBCO_7$ 50 nm film ($\lambda_{PLD}/a = 12$) would require excitations of 10 meV to change the spin state population.

(v) Electron pair states with J = 0, obeying Bose statistics can be formed by the interaction of an O:$2p_{3/2}$ spin defect chain with another of Cu:$3d_{3/2}$ symmetry (and/or Ba:$5d_{3/2}$). The two electron pair states are eigenfunctions of $J = J_1 + J_2$ and J_z but not S_z. The parity of the product states, P for the exchange operation $\mathbf{P}_{12}$ of electrons 1 and 2 of $d_{3/2}$ (Cu or Ba) and $p_{3/2}$ (O) orbital symmetry give the allowed |J,0>:

$\|J,J_z\rangle$		Matrix Coefficients		$d_{3/2}$	$p_{3/2}$	P
$\|3,0\rangle$		$1/40^{1/2}$[1 1 3 3]	$(I+e^{iP}P_{12})$*	$\|3/2\ 1/2\rangle d1$ *	$\|3/2\ -1/2\rangle p2$	2π
$\|2,0\rangle$	=	$1/8^{1/2}$[-1 -1 1 1]	* $(I+e^{iP}P_{12})$*	$\|3/2\ -1/2\rangle d1$ *	$\|3/2\ 1/2\rangle p2$	π
$\|1,0\rangle$		$1/40^{1/2}$[3 3 -1 -1]	$(I+e^{iP}P_{12})$*	$\|3/2\ 3/2\rangle d1$ *	$\|3/2\ -3/2\rangle p2$	2π
$\|0,0\rangle$		$1/8^{1/2}$[1 -1 1 -1]	$(I+e^{iP}P_{12})$*	$\|3/2\ -3/2\rangle d1$ *	$\|3/2\ 3/2\rangle p2$	2π

(6)

where the matrix coefficients are obtained to satisfy the eigenvalues, J(J+1), J_z, and the raising and lowering angular momentum textbook operations [12a]. **I** is the identity operation and electrons 1 and 2 are identified by the position in the product**.** The principal axis of quantization in relation (4) is determined by $\mathbf{k}_{\pm}$ and the electron pair $e_2^{=}$ states allowed by symmetry in (6) are:

$$|0,0\rangle_{ab\ chain} = 5^{-1/2}(\mathbf{I}+\mathbf{P}_{12})\ \{(Y_{1,0\uparrow}\textstyle\sum_n[R_{O:2p}(r-R_{O3a}) - R_{O:2p}(r-R_{O3b})])_1 * (Y_{2,0\downarrow}\ \textstyle\sum_n R_{Cu:3d}(r-R_{Cu}))_2$$

$$- (Y_{1,0\downarrow}\textstyle\sum_n[R_{O:2p}(r-R_{O3a}) - R_{O:2p}(r-R_{O3b})])_1 * (Y_{2,0\uparrow}\ \textstyle\sum_n R_{Cu:3d}(r-R_{Cu}))_2\}. \qquad (7)$$

for J = 0. Bose pairs arising from interactions between electron states in neighboring 1D chains along the diagonal a,b (Fig. 4) mediated by lattice vibrations in $YBCO_7$ of ~ 10 to 80 meV [16b] are possible for J = 3, 1, 0 in (6).

(vi) Equal superconducting properties along the a:b and a:-b diagonals, in a perfect lattice may occur only in a crystal with $\mathbf{k}_+$ and $\mathbf{k}_-$ quantization in two different CuO_2 layers (e.g., $YBCO_7$ Fig. 1a) or when an equal probability of $\mathbf{k}_+$ and $\mathbf{k}_-$ quantization gives rise to bonding $\Leftrightarrow$ anti-bonding excitations of $2t/N \sim 6$ meV, causing the commonly observed PLD.

C. Evidence for magneto-optic effects below T_c has also been obtained in the enhanced 001 scattering by a 50 nm $YBCO_7$ film on $SrTiO_3$ with a 24 DEG grain boundary [8]. Near the Cu $L_{2,3}$ edges both the raw data I_s/I_0 and f" (obtained from the raw data by an inverse Kerr rotation by φ_K =23.5 DEG) indicate below T_c a decrease in the final empty band states contribution of Cu:$3d_{3/2}$ symmetry (L_2 edge) that is greater than for the Cu:$3d_{5/2}$ contribution to the empty final states (L_3 edge) (Fig. 5a). Changes at the O K-edge are difficult to measure because the spin-orbit splitting in the final states bands is negligible (Fig. 5b). However in a film with grain boundaries, electro states are also introduced by broken bonds at the grain boundary in the same manner as when $\mathbf{k}_+$ changes to $\mathbf{k}_-$ (Fig. 4).

5. Conclusions

The temperature dependence of the $YBCO_7$, Ba $L_{2,3}$ XAS indicate that the onset of anti-ferromagnetic optic effects in the Ba layer ~ 10 the K above T_c forecasts the Mott transition [18] associated with the transition to superconductivity. The valence of an alkaline earth metal changes near the metal insulator Mott transition in $Sr(NH_3)_x$ as determined by XAS valence edge shifts [19]. The elegant work of Zhang et al. [20] helps to unravel the $YBCO_7$ superconductivity-magnetism relation. They have shown that spin polarized transport is non-dissipating and that transport by a Bose condensate in the superconducting state is a sub-group of spin polarized transport. A question remains: are the spin polarized $nd_{3/2}$ over the $nd_{5/2}$ band states in $YBCO_7$ a result of the Bose condensation, or does the uneven spin population in nearly 1D conjugate orbitals (5) cause the Bose condensation? Since Faraday rotations are observed above T_c, the latter appears closer to the truth.

6. Acknowledgements

Support for this work was given by an NSF/DMR grant 9612873 at SJSU, and DOE at SSRL. Professor Yao W. Liang of the IRC for superconductivity, Cavendish Laboratory is thanked for the $YBCO_7$ single crystal and for moral support.

7. References

1. P. N. Argyres, *Phys. Rev.* 97, 334 (1955)
2. J.L. Erskine and E.A. Stern, *Phys. Rev.* **B** 12, 5016 (1975)
3. D.T. Cromer and D. A. Lieberman, *Acta Cryst.* A**37**, 267 (1981)
4. J.B. Kortright and M. Rice, *Phys. Rev.* **B** 52, 10240 (1995)
5. J.B. Kortright and S-K Kim, *Phys. Rev.* **B** 62, 12216 (2000)
6. J.V. Acrivos, *Solid State Sciences*, **2**, 807-820 (2000)
7. J.V. Acrivos, L. Nguyen, T. Norman, C.T. Lin, W.Y.Liang, J.M. Honig and Somasundaram, *Microchemical Journal,* **71**, 117-131 (2002)
8. M. A. Navacerrada, H. Sahibuedeen, J.B. Kortright and J.V. Acrivos, *Bulletin of the American Physical Society Meeting: MAR04* **K1.189** (2004), and to be submitted for publication
9. J.B. Kortright, D.D. Awachalom, J. Stohr, S.D. Bader, Y.U. Idzerda, S.S.P. Parkin, I.K. Schuller, and H.C. Seigmann, *J. Magn. Magn. Materials*, **207**, 7-44 (1999).
10. M. A. Navacerrada and J.V. Acrivos, *NanoTech 2003*, **1**, 751 (2003)
11. J.G. Chigvinadze, G.I. Mamniashvilli and J.V. Acrivos, *Bulletin of the American Physical Society Meeting: MAR04,* **K1.189** (2004) and to be submitted for publication.
12. Textbook formulae from: (a) L.I. Schiff, *"Quantum Mechanics"* McGraw Hill, New York 1949, section 239. (b)D. Templeton, *Handbook of Synchrotron Radiation*, **3**, 201 (1991), ed. G. Brown and D.E. Moncton, Elsevier, (c) R.W. James, "The optical principles of X-rays", Ox Bow Press, Woodbridge, Conn. 1962, p. 172; (d) M. E. Rose, *"Elementary Theory of Angular Momentum",* John Wiley and Sons, NY (1953); (e) P.M. Morse and H. Feshbach, "*Methods if Theoretical Physics"*, McGraw Hill, New York (1953); (f) *Handbook of Physics and Chemistry,* R.C. Weast, ed, The Chemical Rubber

Co., D-24 49th Edition (1969); (g) J. Callaway, "Quantum Theory of Solids", Academic Press Inc., San Diego, New York, (1974)

13. J.V. Acrivos and O. Stradella, *International Journal of Quantum Chemistry*, **46**, 55(1993)
14. Z.-X. Shen, W.E. Spicer, D.M. King, D.S. Dessau, B.O.Wells, *Science* **267**, 343 (1995)
15. R. Pauncz, *"Fundamental World of Quantum Chemistry"*, E.J. Brändas and E.S. Kryachko ed., Kluwer Academic Pub. Dordrecht, p. 155 (2003)
16. (a) N. Watanabe and N. Koshizuka, *Advances in Superconductivity **IX**,* p. 153 , Springer-Verlag, Tokyo (1997); (b) C. Thomsen and M. Cardona, *Physical Properties of High Tc Superconductors **I,*** p. 409 (1988), World Scientific, D. M. Ginsberg, ed
17. H.S.Sahibudeen and J.V. Acrivos, *227th ACS National Meeting, Anaheim, CA, March 28-April 1, 2004* **INOR 588**, (2004) and to be submitted for publication
18. N.F. Mott, "Metal Insulator Transitions", Taylor and Francis, ltd, 1974
19. J.V. Acrivos, K. Hathaway, A. Robertson, and M.P. Klein, *J. Phys. Chem.* 84, 1206 (1980).
20. S. Murakami, N. Nagaosa and S. C. Zhang, *Science* **301**, 1348 (2003)

8. List of Figures

Fig.1: Schematic of sample and measurement parameters: (a) $YBCO_7$ crystal structure. **(b)** CuO_2 conduction layer intercalated between Ba and Y donor layers. **(c)** Scattered, I_s and transmitted, I_T beams of incident radiation, I_0 by sample. I_s/I_0 and I_T/I_0 measure the change in the initial state $|\mathbf{k,g}>$ produced by complicated reflection and transmission operators $\mathbf{R}$ and $\mathbf{T}$ [ref. 1-5, 12]. $\theta' = \mathbf{c}\hat{}\boldsymbol{\varepsilon}_{X\text{-}rays} = 8\pi/18$ and $\theta = = \mathbf{k_i}\hat{}\mathbf{a}$ where $\mathbf{k}_i$ is the direction of incident X-rays and $\boldsymbol{\varepsilon}_{X\text{-}rays}$ the direction of their linear polarization and **g** represents the quantum state of the system.

Fig.2: Ba $L_{2,3}$ edge XAS for $YBCO_7$ single crystal. $A(T)/A(121\ K)$ at the orientation $\theta = 8\pi/18$ near T_c of YBCO single Crystal of 22 μm thick [ref. 6,7]. The raw data is corrected only for baseline (indicated in insert). The ratio $A(T)/A(121\ K)$ eliminates the effect of sample thickness, except for the magneto-optic effects. $A(T)/A(121\ K)$ does not change appreciably from room temperature to 56K at $\theta = \pi/2$, but at $\theta = 8\pi/18$ the complex index of refraction indicates the presence of magneto-optic effects 10 K above T_c. The transmission (Fig. 1c) vanishes in the interval ΔE near the indicated resonance absorptions, and depend on T (inserts).

Fig. 3: $(CuO_2)_n$ electron density contours of $\rho_e > 10^{-3}/bohr^3$ obtained for a T'-Nd_2CuO_4 nano-particle in the field of 18 unit cells [13]: (a) $Cu_4O_4{:}\chi_{m,74}$ **(b)** $Cu_4O_{12}{}^{-x}{:}\chi_{m',114}$ **(c)** Tight binding SCF-MO approximation for $\mathbf{k}_+ = (\pi, \pi, 0)$:

$$\Psi_{m'm}(\mathbf{r}, \mathbf{k}) = N^{-1/2}\Sigma_R \{\exp(i\,\mathbf{k}\cdot\mathbf{R_{74}})\ \chi_{m,74}(\mathbf{r}-\mathbf{R_{74}}) + \exp(i\,\mathbf{k}\cdot\mathbf{R_{114}})\ \chi_{m',114}(\mathbf{r}-\mathbf{R_{114}})\} =$$

$$\Psi_{m'm}(\mathbf{r},(\pm\pi,\pm\pi, 0)) = 1/\sqrt{N}\ \Sigma_{Ri}\ \{\chi_{m,74}\ (\mathbf{r}-R_{74}) + \chi_{m',114}\ (\mathbf{r}-R_{114})\},$$

n = 0, 1,. N/2 and the MO are centered at: $\mathbf{R_{114}} = 2\ n(\mathbf{a} \pm \mathbf{b})$ and $\mathbf{R_{74}} = 2\ (n\ \mathbf{a} \pm (n-1)\ \mathbf{b})$.

Fig. 4: Direction of extended orbital overlap population in conjugate MO in the CuO_2 plane for $\mathbf{k}_{\pm}$. The $O_{3a}{:}2p_{ab}$-O3b:$2p_{ab}$ overlap is indicated by solid lines (for + 2p orbital phase) and dashed lines (for - 2p orbital phase). The Cu:3d phase is indicated by solid lines (+) and dashed

lines (-) respectively. Anti-bonding states are created where k_+ changes to k_- (blank). The PLD periodicity is produced by the repeat chevron symmetry.

Fig. 5: Enhanced 001 scattering by 50 nm $YBCO_7$, film on $SrTiO_3$ with a 24 DEG grain boundary according to ref. 8: (a) f" near the Cu $L_{2,3}$ edges at different T above and below T_c. **(b)** f" near the O K edge at different T above and below T_c.

Figure 1a:

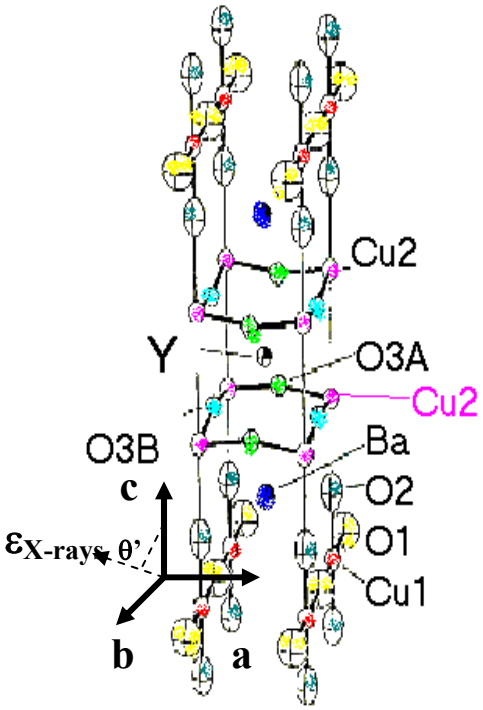

Figure 1b:

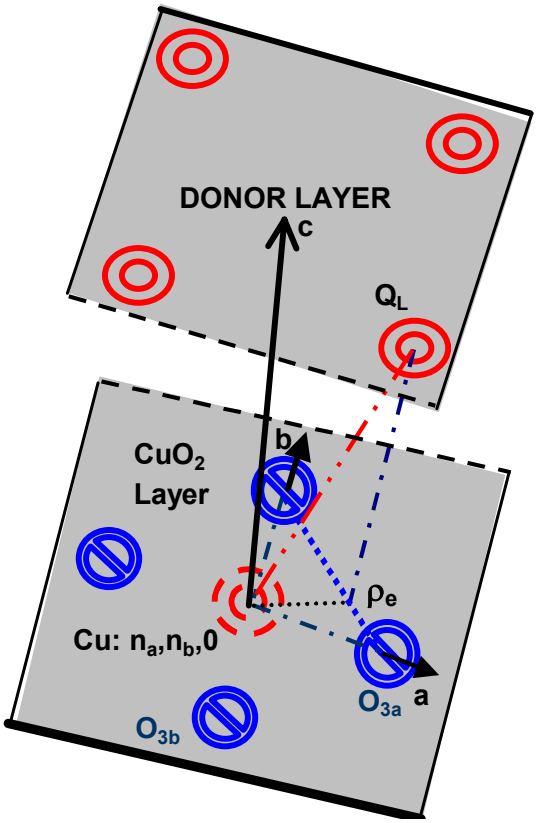

Figure 1c:

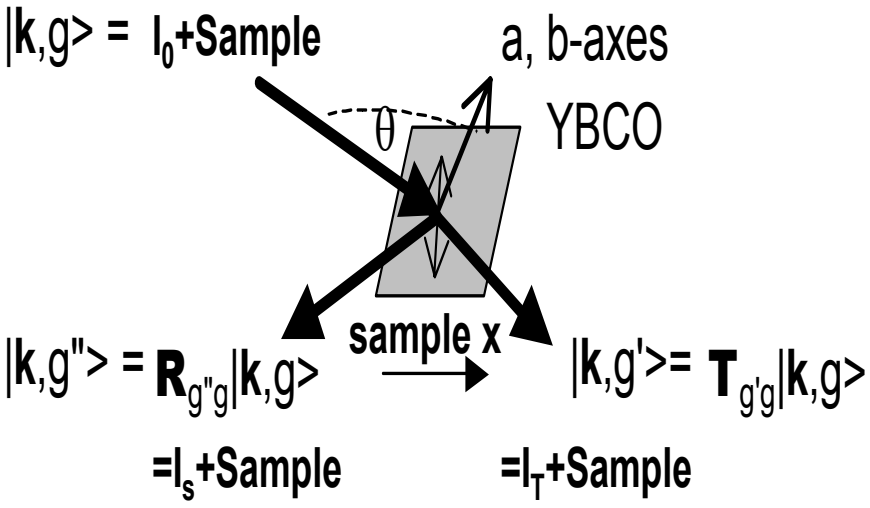

Fig. 2

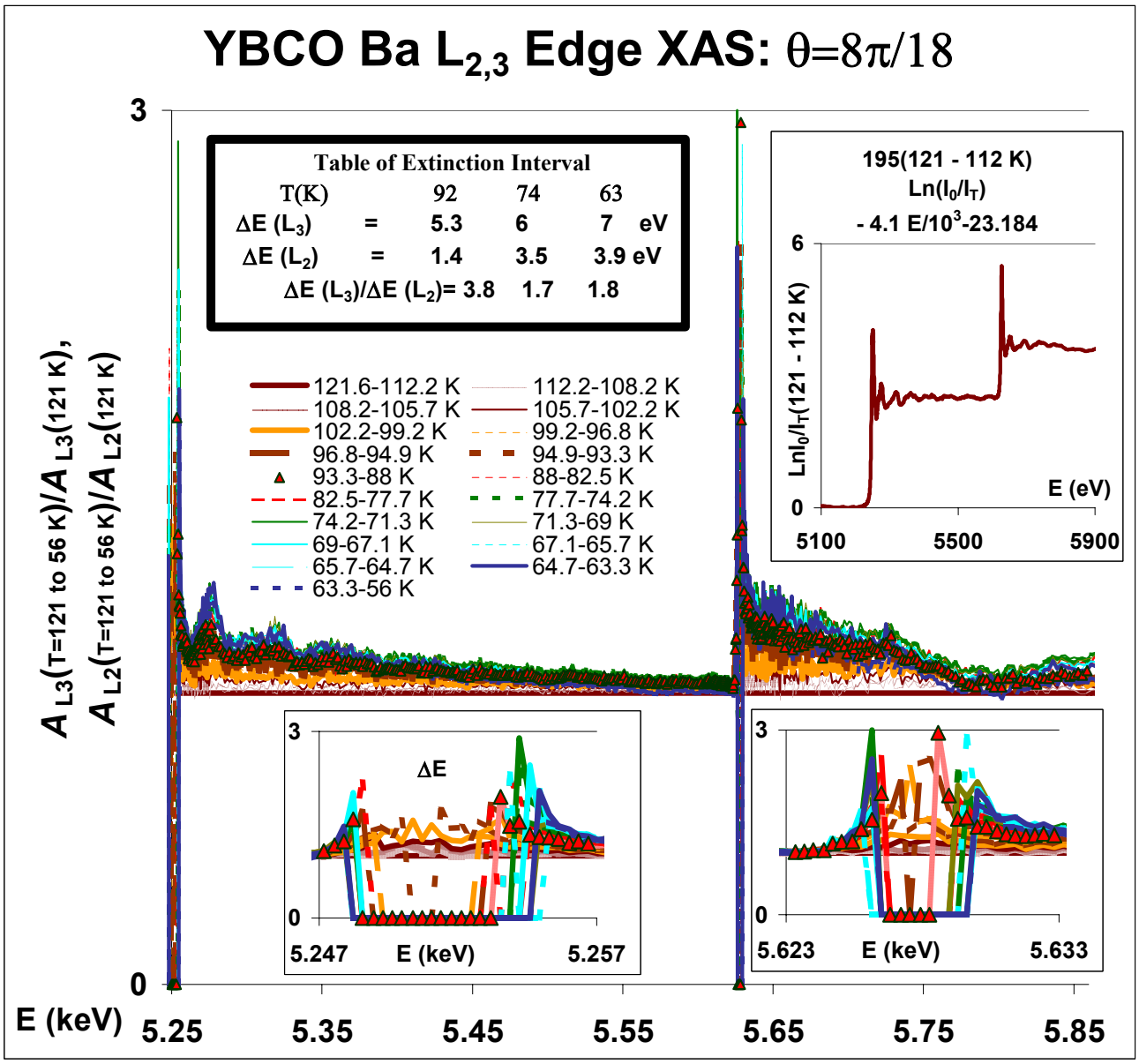
YBCO Ba L2,3 Edge XAS: θ=8π/18
Table of Extinction Interval
T(K) 92 74 63
ΔE (L3) = 5.3 6 7 eV
ΔE (L2) = 1.4 3.5 3.9 eV
ΔE (L3)/ΔE (L2)= 3.8 1.7 1.8
121.6-112.2 K
112.2-108.2 K
108.2-105.7 K
105.7-102.2 K
102.2-99.2 K
99.2-96.8 K
96.8-94.9 K
94.9-93.3 K
93.3-88 K
88-82.5 K
82.5-77.7 K
77.7-74.2 K
74.2-71.3 K
71.3-69 K
69-67.1 K
67.1-65.7 K
65.7-64.7 K
64.7-63.3 K
63.3-56 K
195(121 - 112 K)
Ln(I0/IT)
- 4.1 E/10^3-23.184
LnI0/IT(121 - 112 K)
E (eV)
ΔE
E (keV)
A L3(T=121 to 56 K)/A L3(121 K),
A L2(T=121 to 56 K)/A L2(121 K)

Figure 3a:

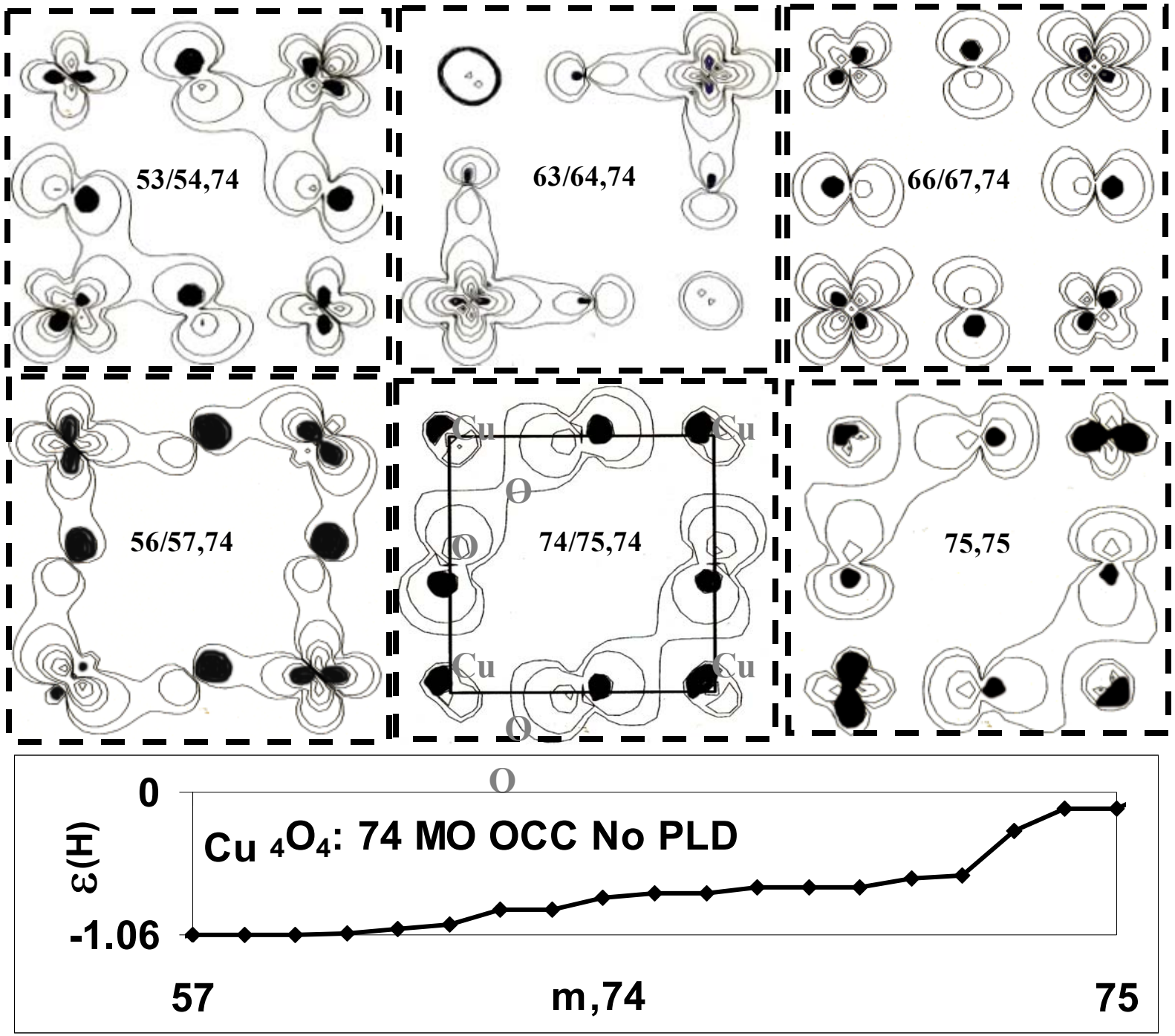
53/54,74
63/64,74
66/67,74
56/57,74
Cu
Cu
O
O
74/75,74
Cu
Cu
O
75,75
O
0
ε(H)
Cu 4O4: 74 MO OCC No PLD
-1.06
57
m,74
75

Figure 3b:

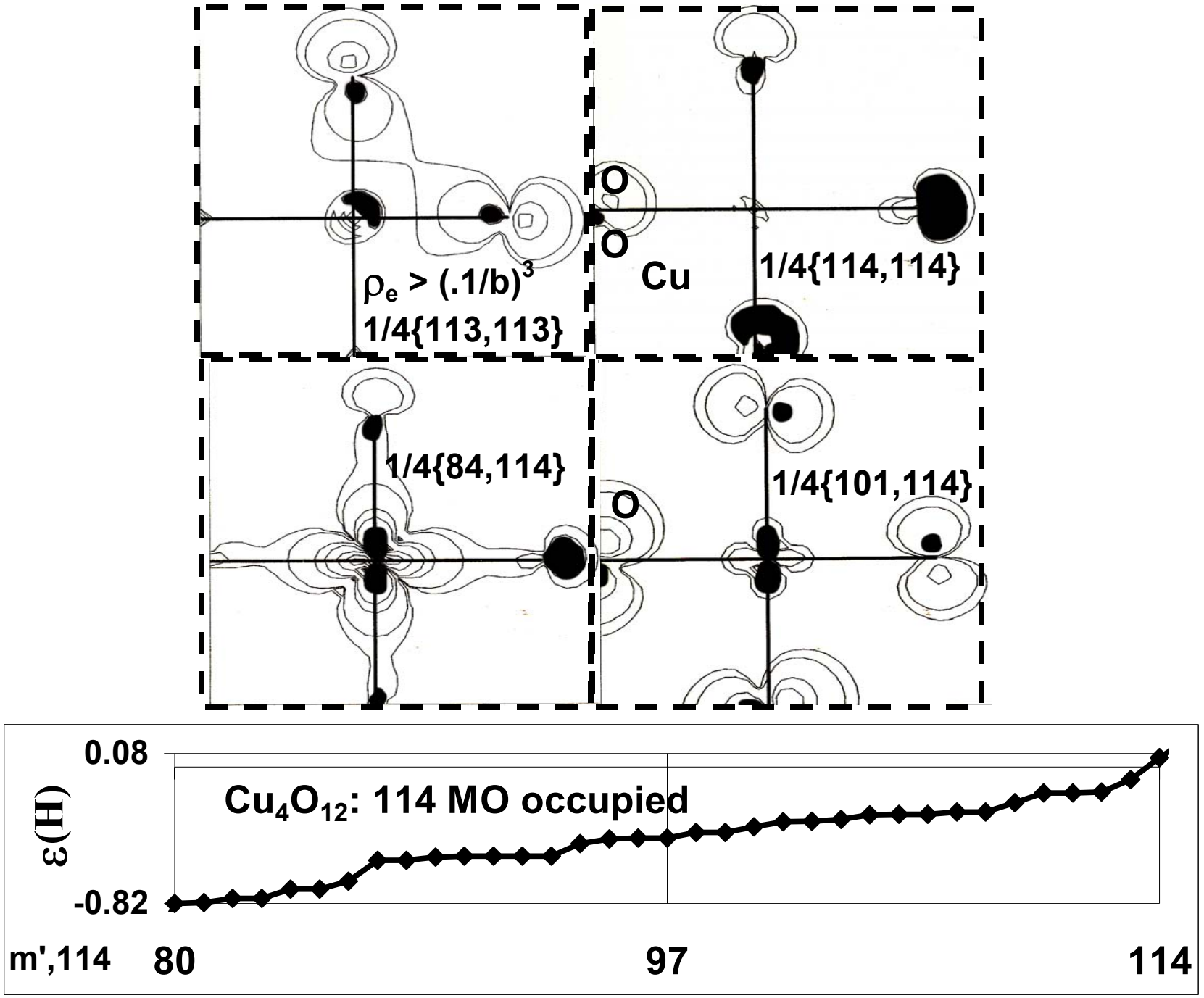
$\rho_e > (.1/b)^3$
1/4{113,113}
O
O
Cu
1/4{114,114}
1/4{84,114}
O
1/4{101,114}
0.08
Cu_4O_{12}: 114 MO occupied
ε(H)
-0.82
m',114
80
97
114

Figure 3c:

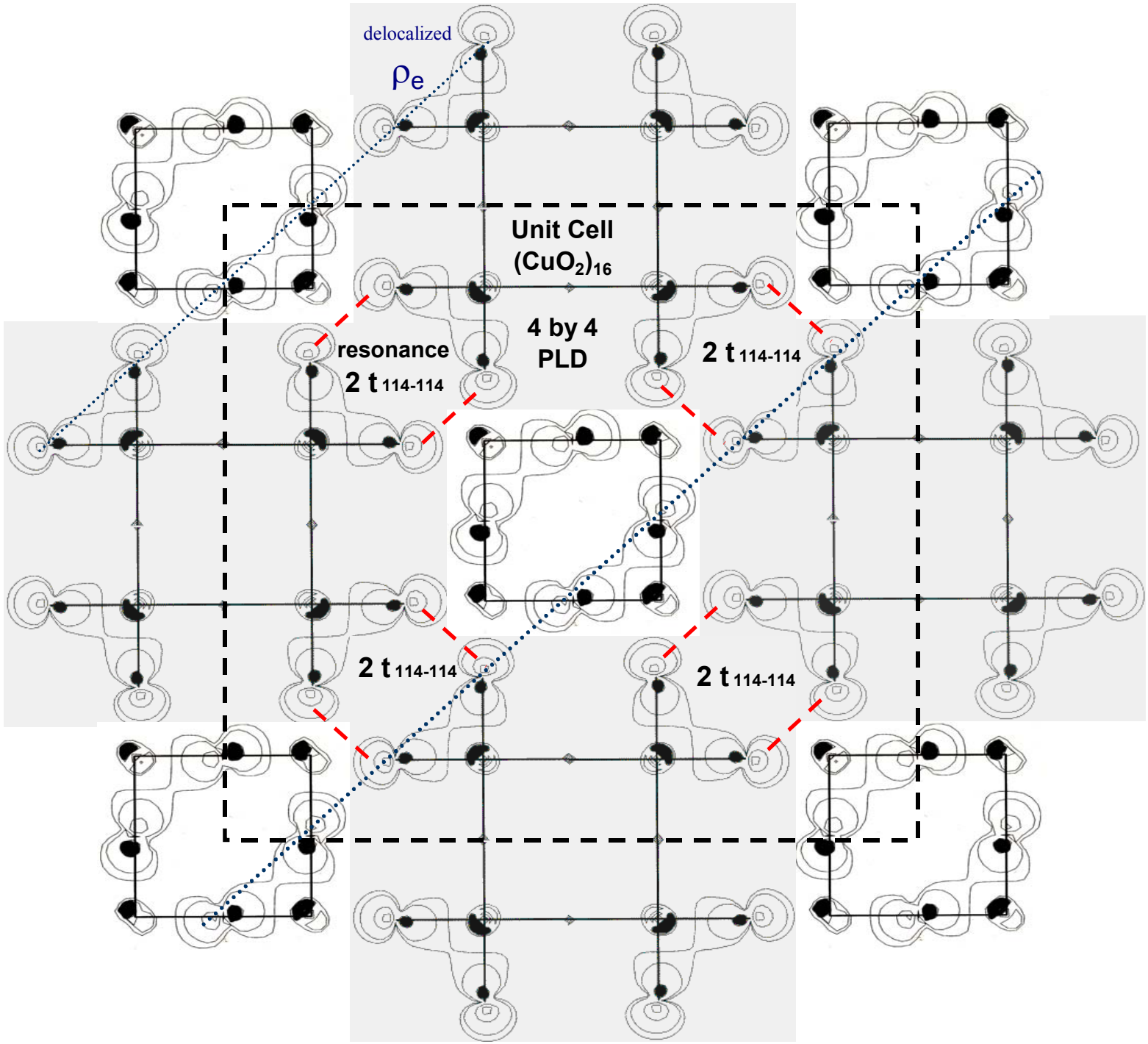
delocalized
ρ_e
Unit Cell
$(CuO_2)_{16}$
4 by 4
PLD
resonance
2 t 114-114
2 t 114-114
2 t 114-114
2 t 114-114

Figure 4:

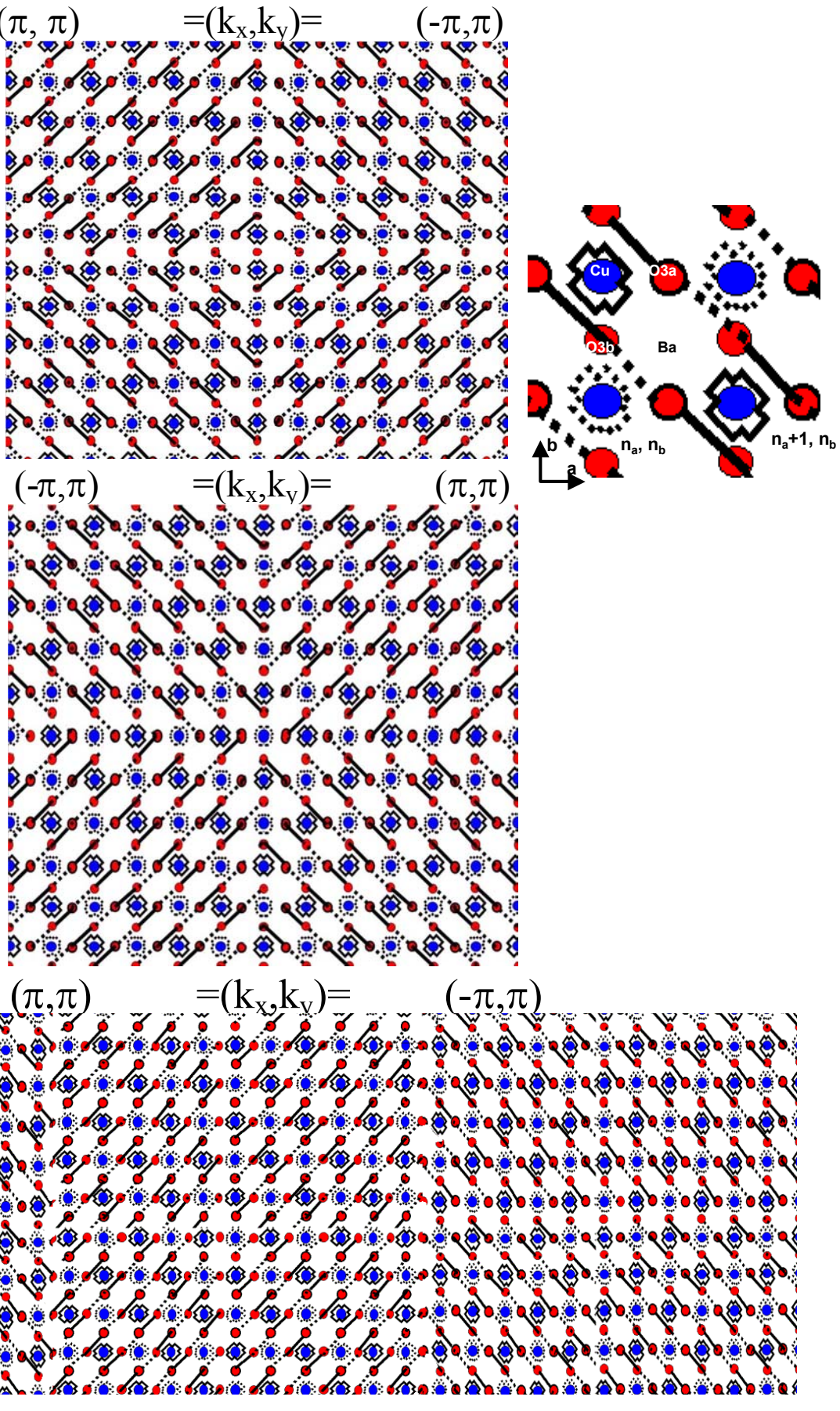

Fig. 5a:

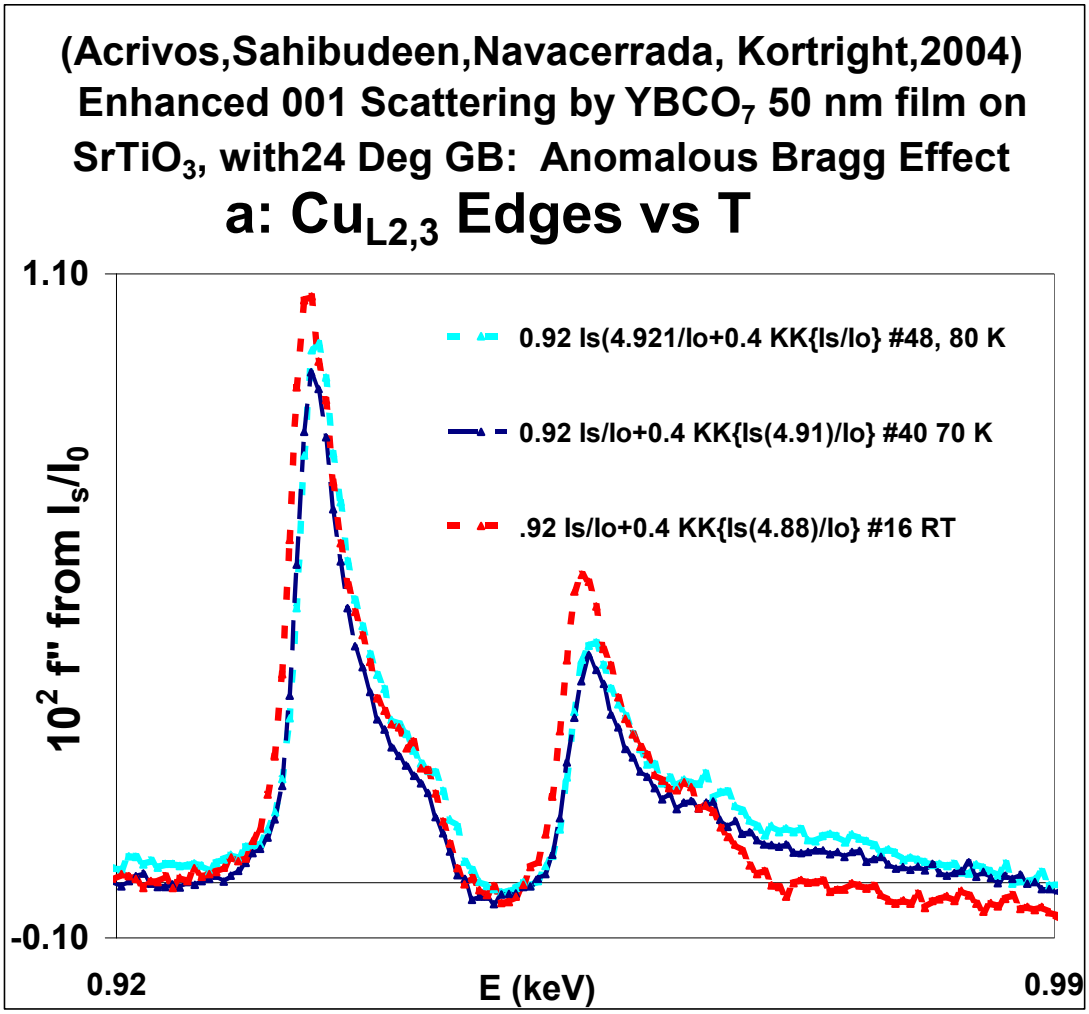
(Acrivos,Sahibudeen,Navacerrada, Kortright,2004)
Enhanced 001 Scattering by YBCO7 50 nm film on SrTiO3, with24 Deg GB: Anomalous Bragg Effect
a: CuL2,3 Edges vs T
1.10
-0.10
10^2 f" from Is/Io
0.92 Is(4.921/Io+0.4 KK{Is/Io} #48, 80 K
0.92 Is/Io+0.4 KK{Is(4.91)/Io} #40 70 K
.92 Is/Io+0.4 KK{Is(4.88)/Io} #16 RT
0.92
E (keV)
0.99

Fig. 5b:

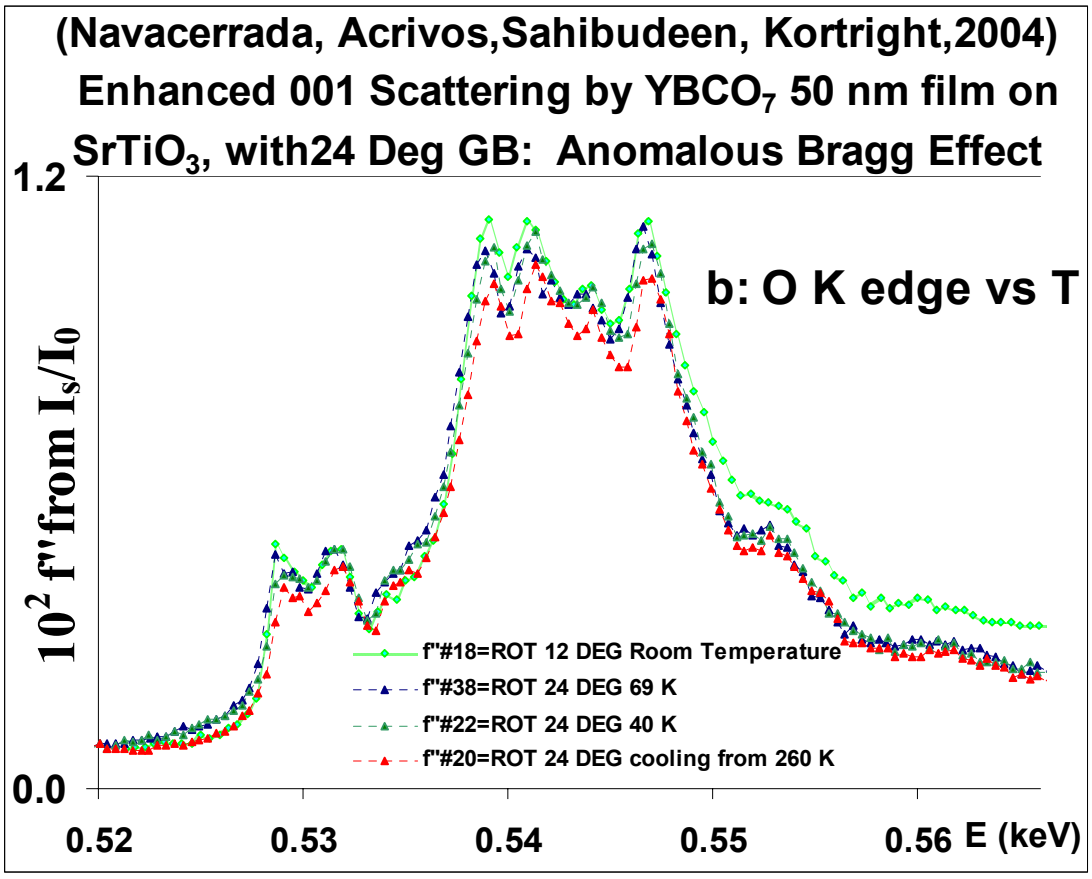
(Navacerrada, Acrivos,Sahibudeen, Kortright,2004)
Enhanced 001 Scattering by YBCO7 50 nm film on SrTiO3, with24 Deg GB: Anomalous Bragg Effect
1.2
0.0
10^2 f''from Is/Io
b: O K edge vs T
f"#18=ROT 12 DEG Room Temperature
f"#38=ROT 24 DEG 69 K
f"#22=ROT 24 DEG 40 K
f"#20=ROT 24 DEG cooling from 260 K
0.52
0.53
0.54
0.55
0.56
E (keV)